

## 2.5. TWO-DIMENSIONAL POWDER DIFFRACTION

## 2.5.4. Applications

## 2.5.4.1. Phase identification

In materials science, a phase is defined as a region that has uniform chemical composition and physical properties, including crystal structure. Therefore, every phase should give a unique diffraction pattern. A sample for X-ray diffraction may contain a single phase or multiple phases. Analysis of the diffraction pattern can accurately and precisely determine the contents of the sample. This qualitative analysis is called phase identification (phase ID). One of the most efficient methods of phase identification is to compare the diffraction pattern from an unknown material to those in a database of a large number of standard diffraction patterns. The most comprehensive database is the Powder Diffraction File (PDF), updated annually by the International Centre for Diffraction Data (ICDD).

Two-dimensional X-ray diffraction has enhanced phase identification in many respects (Rudolf & Landes, 1994; Sulyanov *et al.*, 1994; Hinrichsen, 2007). Because of its ability to collect diffracted X-rays in a large angular range in both the  $2\theta$  and  $\gamma$  directions, it can collect diffraction data with high speed and better sampling statistics than obtained by conventional diffraction. Owing to point-beam illumination on the sample, a relatively small sample size is required for phase identification. The large 2D detector allows for a large  $2\theta$  range to be analysed without any movement of the sample and detector. This makes it possible to perform *in situ* phase investigation on samples during phase transformations, chemical reactions and deformations. The diffraction information in the  $\gamma$  direction allows accurate phase identification of samples with large grains and preferred orientation.

In the Bragg–Brentano geometry, the  $2\theta$  resolution is controlled by the selection of the divergence slit and receiving slit in the diffractometer plane, and the axial divergence is controlled by Soller slits, while in a diffractometer with a 2D detector, the  $2\theta$  resolution is mainly determined by the spatial resolution of the detector and the sample-to-detector distance. The relative peak intensity in a diffraction pattern from a sample with texture measured with a 2D detector can be significantly different from the results measured with Bragg–Brentano geometry. It is imperative to study the nature of these discrepancies so that the diffraction patterns collected with 2D detectors can be used for phase ID with proper understanding and correction if necessary.

When two-dimensional diffraction is used for phase identification, the first step is to integrate the 2D diffraction frame into a diffraction profile resembling the diffraction pattern collected with a conventional diffractometer (Cervellino *et al.*, 2006; Rodriguez-Navarro, 2006; Boesecke, 2007; Fuentes-Montero *et al.*, 2011; Hammersley, 2016). The integrated diffraction profiles can be analysed with all existing algorithms and methods, including profile fitting with conventional peak shapes and fundamental parameters, quantification of phases, and lattice-parameter determination and refinement (Ning & Flemming, 2005; Flemming, 2007; Jabeen *et al.*, 2011). The results can be used to search a powder-diffraction database to find possible matches. Since there is a great deal of literature covering these topics (Cullity, 1978; Jenkins & Snyder, 1996; Pecharsky & Zavalij, 2003), this section will focus on the special characteristics of two-dimensional X-ray diffraction as well as system geometry, data-collection strategies and data analysis in dealing with relative peak intensities,  $2\theta$  resolution, grain size and distribution, and preferred orientation. Many factors and correction algorithms described here can help in understanding the character-

istics of two-dimensional diffraction. In most applications, however, the  $\gamma$ -integrated profile can be used for phase identification without these corrections.

## 2.5.4.1.1. Relative intensity

The integrated intensity diffracted from polycrystalline materials with a random orientation distribution is given by

$$I_{hkl} = k_I \frac{p_{hkl}}{v^2} (\text{LPA}) \lambda^3 F_{hkl}^2 g_{hkl}(\alpha, \beta) \exp(-2M_t - 2M_s), \quad (2.5.45)$$

where  $k_I$  is an instrument constant that is a scaling factor between the experimental observed intensities and the calculated intensity,  $p_{hkl}$  is the multiplicity factor of the crystal plane ( $hkl$ ),  $v$  is the volume of the unit cell, (LPA) is the Lorentz–polarization and absorption factors,  $\lambda$  is the X-ray wavelength,  $F_{hkl}$  is the structure factor for the crystal plane ( $hkl$ ),  $g_{hkl}(\alpha, \beta)$  is the normalized pole-density distribution function and  $\exp(-2M_t - 2M_s)$  is the attenuation factor due to lattice thermal vibrations and weak static displacements (Warren, 1990; He *et al.*, 1994). Except for the texture effect, all the factors in the above equation are either discussed in the previous sections or have the same definitions and values as in conventional diffraction.

Phase-identification studies by XRD are preferably carried out on powders or polycrystalline samples with a random orientation distribution of crystallites. Preferred orientation causes relative intensities to deviate from theoretical calculations or those reported in reference databases. In practice, a sample with a perfectly random orientation distribution of crystallites is very hard to fabricate and most polycrystalline samples have a preferred orientation to a certain extent. Discrepancies in the relative peak intensities between conventional diffraction and 2D-XRD are largely due to texture effects. For B-B geometry, the diffraction vector is always perpendicular to the sample surface. With a strong texture, it is possible that the pole density of certain reflections in the sample normal direction is very low or even approaches zero. In this case, the peak does not appear in the diffraction pattern collected in B-B geometry. In 2D-XRD, several diffraction rings may be measured with a single incident beam; the corresponding diffraction vectors are not necessarily in the sample normal direction. The diffraction profiles from 2D frames are produced by  $\gamma$  integration, therefore the texture factor  $g_{hkl}(\alpha, \beta)$  should be replaced by the average normalized pole-density function within the  $\gamma$  integration range ( $g_{hkl}(\Delta\gamma)$ ). The relation between  $(\alpha, \beta)$  and  $(2\theta, \gamma)$  is given in Chapter 5.4. The chance of having zero pole density over the entire  $\gamma$ -integration range is extremely small. Therefore, phase identification with 2D-XRD is much more reliable than with conventional diffraction.

## 2.5.4.1.2. Detector distance and resolution

The  $2\theta$  resolution with B-B geometry is controlled by the size of the slits. Smaller apertures of the divergence slit are used for higher  $2\theta$  resolution and larger apertures for fast data collection. With a two-dimensional X-ray diffraction system, the  $2\theta$  resolution is achieved with different approaches. A flat 2D detector has the flexibility to be used at different sample-to-detector distances. The detector resolution is determined by the pixel size and point-spread function. For the same detector resolution and detector active area, a higher resolution can be achieved at larger distance, and higher angular coverage at shorter distance. The sample-to-detector distance should be optimized depending on the  $2\theta$  measurement range and required resolution. In situations where the  $2\theta$  range of one frame is not enough, several frames at

## 2. INSTRUMENTATION AND SAMPLE PREPARATION

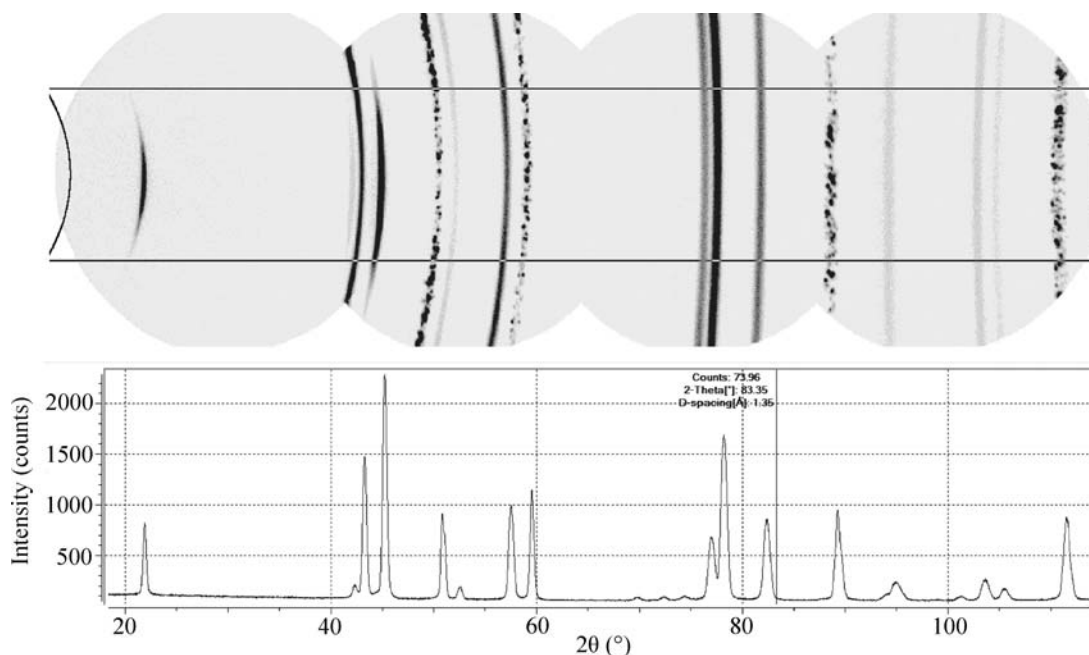


**Figure 2.5.16**  
Diffraction pattern merged from four 2D frames collected from a battery material.

sequential  $2\theta$  ranges can be collected. The integrated profiles can then be merged to achieve a large  $2\theta$  range. Fig. 2.5.16 shows four 2D frames collected from a battery material with a microgap detector. The slice integration region is defined by two conic lines and two horizontal lines. The diffraction profile integrated from the merged frames is displayed below.

### 2.5.4.1.3. Defocusing effect

A 2D diffraction pattern over a range of  $2\theta$  is measured simultaneously with a single incident angle, so the incident angle has to be lower than the minimum  $2\theta$  angle. Since the reflected angle cannot always be the same as the incident angle, geometric aberrations are observed. The defocusing effect occurs when the incident angle is lower than the reflection angle. At low incident angles, the incident beam spreads over the sample surface into an area much larger than the size of the original X-ray beam. The observed diffracted beam size is magnified by the defocusing effect if the diffracted beam makes an angle larger than the incident angle. The defocusing effect for reflection-mode diffraction can be expressed as

$$\frac{B}{b} = \frac{\sin \theta_2}{\sin \theta_1} = \frac{\sin(2\theta - \omega)}{\sin \omega}, \quad (2.5.46)$$

where  $\theta_1$  is the incident angle,  $b$  is the incident beam size and  $B$  is diffracted beam size. The ratio of  $B$  to  $b$  is a measurement of the geometric aberration and will be referred to as the defocusing factor. In principle, defocusing occurs only when  $B/b$  is larger than 1. The reflected beam is actually focused to the detector when  $\theta_2 < \theta_1$ . The defocusing effect occurs when  $\theta_2 > \theta_1$  and the defocusing factor increases with increasing  $\theta_2$  or decreasing  $\theta_1$ . The maximum defocusing appears at  $\theta_2 = 90^\circ$ . For the  $\theta$ - $2\theta$  configuration, the incident angle  $\omega (= \theta_1)$  is used in the equation.

For B-B geometry with a divergent slit and receiving slit of the same size the defocusing factor is always 1. With a 2D detector the defocusing factor varies with the  $2\theta$  angle. If a large  $2\theta$  range is measured on a flat sample in reflection mode, it is always desirable to collect several frames at different incident angles for each  $2\theta$  range so as to improve the  $2\theta$  resolution. A cylindrical

detector may collect a diffraction pattern over a large  $2\theta$  range (Gelfi *et al.*, 2005). However, the defocusing effect prevents it from being used for a large  $2\theta$  range for a flat sample. Fig. 2.5.17 compares the effect for a flat detector and a cylindrical detector. Fig. 2.5.17(a) shows a cylindrical detector being used to collect a diffraction pattern from a flat sample for a  $2\theta$  range of 5 to  $80^\circ$ . The incident angle must be kept at  $5^\circ$  or lower. Fig. 2.5.17(b) shows a flat detector being used to collect the diffraction pattern over the same  $2\theta$  range. In order to minimize the defocusing effect, the data collection is done at four different incident angles ( $5^\circ$ ,  $15^\circ$ ,  $25^\circ$  and  $35^\circ$ ) with four corresponding detector swing angles ( $10^\circ$ ,  $30^\circ$ ,  $50^\circ$  and  $70^\circ$ ). Fig. 2.5.17(c) compares the defocusing factors of the two configurations. The horizontal dot-dashed line with defocusing factor  $B/b = 1$  represents the situation with B-B geometry. The defocusing factor continues to increase with  $2\theta$  angle up to  $B/b = 11$  for cylindrical detector. That means that the  $2\theta$  resolution would be 10 times worse than for the B-B geometry. For the diffraction pattern collected with a flat detector in four steps, the defocusing factor fluctuates above 1, with the worst value being less than 3. Another approach to avoiding defocusing is to collect the diffraction pattern in transmission mode. There is no defocusing effect in transmission when the incident beam is perpendicular to the sample surface. Therefore, the transmission pattern has significantly better  $2\theta$  resolution. Transmission-mode diffraction also has other advantages. For instance, the air scattering from the primary beam may be blocked by a flat sample, therefore lowering the background from air scattering. However, transmission-mode diffraction data can only be collected from samples with limited thickness, and the maximum scattering intensity is achieved at low  $2\theta$  angles with a sample thickness of  $t = 1/\mu$ , where  $\mu$  is the linear absorption coefficient. The scattering intensity drops dramatically when the thickness increases.

### 2.5.4.1.4. Sampling statistics

In powder X-ray diffraction, the number of crystallites contributing to each reflection must be sufficiently large to generate reproducible integrated peak intensities (see Chapter 2.10). A larger number of contributing crystallites gives better precision or sampling statistics (also referred to as particle